Overexpression of Foxc1 ameliorates sepsis-associated encephalopathy by inhibiting microglial migration and neuroinflammation through the IκBα/NF-κB pathway

HONGYU WANG[1-3], HONGWEI WANG[4], YINSEN SONG[2,3], CONGYAN LIU[3], XINLING QIAN[2,3], DALONG ZHANG[2,3], XIN JIANG[2,3] and SISEN ZHANG[1-3]

[1]Department of Critical Care Medicine, The Second School of Clinical Medicine, Southern Medical University, Guangzhou, Guangdong 510280; [2]Department of Emergency Medicine, People's Hospital of Henan University of Chinese Medicine/Zhengzhou People's Hospital; [3]Department of Critical Care Medicine, The Fifth Clinical Medical College of Henan University of Chinese Medicine, Zhengzhou, Henan 450003; [4]Department of Respiratory Medicine, Xinhua Hospital, School of Medicine, Shanghai Jiao Tong University, Shanghai 200092, P.R. China

Received August 12, 2021; Accepted December 30, 2021

DOI: 10.3892/mmr.2022.12623

Abstract. Sepsis-associated encephalopathy (SAE) is a common and severe complication of sepsis. The cognitive dysfunction that ensues during SAE has been reported to be caused by impairments of the hippocampus. Microglia serves a key role in neuroinflammation during SAE through migration. Forkhead box C1 (Foxc1) is a member of the forkhead transcription factor family that has been found to regulate in cell migration. However, the role of Foxc1 in neuroinflammation during SAE remains unknown. In the present study, the mechanistic role of Foxc1 on microglial migration, neuroinflammation and neuronal apoptosis during the occurrence of cognitive dysfunction in SAE was investigated. A microglia-mediated inflammation model was induced by LPS in BV-2 microglial cells *in vitro*, whilst a SAE-related cognitive impairment model was established in mice using cecal ligation and perforation (CLP) surgery. Cognitive function in mice was evaluated using the Morris Water Maze (MWM) trial. Lipopolysaccharide (LPS) treatment was found to trigger BV-2 cell migration, inflammation and neuronal apoptosis. In addition, CLP surgery induced cognitive injury, which was indicated by longer latencies and shorter dwell times in the goal quadrant compared with those in the Sham group in the MWM trial. LPS treatment or CLP induction decreased the expression of Foxc1 and inhibitor of NF-κB (IκBα) whilst increasing that of p65, IL-1β and TNF-α. After Foxc1 was overexpressed, the cognitive dysfunction of mice that underwent CLP surgery was improved, with the expression of IκBα also increased, microglial cell migration, the expression of p65, IL-1β and TNF-α and neuronal apoptosis were all decreased *in vivo* and *in vitro*, which were in turn reversed by the inhibition of IκBα *in vitro*. Overall, these results suggest that the overexpression of Foxc1 inhibited microglial migration whilst suppressing the inflammatory response and neuronal apoptosis by regulating the IκBα/NF-κB pathway, thereby improving cognitive dysfunction during SAE.

Correspondence to: Professor Sisen Zhang, Department of Critical Care Medicine, The Second School of Clinical Medicine, Southern Medical University, 1023-1063 Shatai South Road, Baiyun, Guangzhou, Guangdong 510280, P.R. China
E-mail: 2362176700@qq.com

Dr Hongwei Wang, Department of Respiratory Medicine, Xinhua Hospital, School of Medicine, Shanghai Jiao Tong University, 1665 Kongjiang Road, Yangpu, Shanghai 200092, P.R. China
E-mail: 401283662@qq.com

Key words: sepsis-associated encephalopathy, forkhead box C1, migration, microglia, neuroinflammation, IκBα/NF-κB pathway

Introduction

Cognitive dysfunction as a result of sepsis-associated encephalopathy (SAE) is a serious complication of sepsis (1). Lipopolysaccharide (LPS)-activated macrophages can directly permeate into the central nervous system (CNS) to produce an inflammatory response. In addition, LPS can indirectly produce neuroinflammation by peripheral inflammatory factors diffusing into the CNS through the blood-brain barrier, thus leading to CNS inflammatory injury (1). Symptoms of SAE-related cognitive dysfunction ranges from mild delirium to coma, which can persist for months to years (2). They are frequently associated with reduced quality of life and poor prognosis, in addition to increased morbidity and mortality (3). Several studies previously revealed that cognitive dysfunction is associated with microglial activation and hypoxic-ischemic injury, which then activates the inflammatory response in the hippocampus (4,5). This leads to pathological changes that are comparable to those observed during neurodegenerative diseases (6,7). However, the specific mechanism of this remains elusive.

The pathogenesis of SAE involves a number of factors, including neuroinflammation, collapse of the blood brain barrier (BBB), ischemic injury, alterations in the neurotransmitter profile and mitochondrial dysfunction. Aberrant neuroinflammation has been reported to at least in part mediate the pathogenesis of SAE and multiple organ dysfunction syndrome (MODS) (8,9). This is especially the case for the CNS injury that occurs during MODS, which is vulnerable to inflammatory insults (8,9). Additionally, neuroinflammation has been previously found to be responsible for the extensive apoptosis of various cell types in the brain, including microglial cells, neurons and vascular endothelial cells (10). Microglia-mediated neuroinflammation reportedly mediates a substantial portion of the inflammatory response in the CNS, which results in worse outcomes due to septic complications (11-13).

Forkhead box C1 (Foxc1) is a transcription factor that is involved in various pathophysiological processes, such as myocardial ischemia (14), facial paralysis (15) and colorectal cancer (16). Recent studies revealed that Foxc1 can promote defense against oxidative stress, inflammation and apoptosis (17,18). In addition, Foxc1 has been found to serve key roles in a number of biological processes, including cell proliferation, differentiation, migration and survival (19,20). A previous study demonstrated that upregulation of Foxc1 expression promoted Schwann cell migration (15). By contrast, knockdown of Foxc1 expression has been shown to significantly suppress the migration of cervical and breast cancer cells (21,22). In terms of myeloid tissue regeneration, Foxc1 was demonstrated to promote regenerative functions by promoting mveloid tissue bone marrow mesenchymal stem cell migration (23). However, the biological function of Foxc1 in microglial cells remains poorly understood.

NF-κB consists of a family of transcription factors that are involved in the regulation of inflammation, cell proliferation, migration, differentiation and survival (24,25). NF-κB can regulate the expression of genes involved in a wide range of biological processes, including cancer cell proliferation, migration and apoptosis (25). A previous study has revealed that suppression of NF-κB signaling can attenuate inflammation and cell migration in LPS-treated BV-2 microglial cells (26). However, the relationship between Foxc1 and the NF-κB pathway in microglial physiology remains unclear.

In the present study, the potential role of Foxc1 in SAE-associated cognitive dysfunction was investigated using an LPS-induced microglial cell model and a cecal ligation and perforation (CLP) mouse model. In addition, the effects of Foxc1 on microglial migration in the hippocampus and NF-κB signaling were also focused upon. These results may prove beneficial for the development of therapeutic strategies for SAE.

Materials and methods

Cell culture and treatment. BV-2 is a murine-derived immortalized microglial cell line and were purchased from ScienCell Research Laboratories, Inc., which were routinely cultured in DMEM (Gibco; Thermo Fisher Scientific, Inc.) supplemented with 10% FBS (Gibco; Thermo Fisher Scientific, Inc.) and 2 mM L-glutamine, penicillin (100 U/ml) and streptomycin (100 g/ml; Invitrogen; Thermo Fisher Scientific, Inc.) at 37˚C with 5% CO_2 and 95% humidity. For treatment, BV-2 cells were incubated in a six-well plate at a density of $1x10^5$ cells/ml at 37˚C with 5% CO_2 for 24 h, and were then cultured in the absence or presence of 100 ng/ml LPS (Sigma-Aldrich; Merck KGaA) for 6 h (27).

Foxc1 adenovirus transfection. Foxc1 adenovirus (Ad-Foxc; adenoviral plasmid name: GV345; target gene ID: 17300; sequence: GGTATAAGAGGCGCGACCAG; accession no. NC_000079; $4x10^8$ TU/ml; Shanghai GeneChem Co., Ltd.) or the adenovirus control (Ad-Ctrl), which is the adenovirus containing the empty vector without the Foxc1 gene ($1.5x10^9$ TU/ml; Shanghai GeneChem Co., Ltd.), was added into the media for transfection into BV-2 cells at a 60-80% confluence. Transfection was for 8 h at 37˚C with 5% CO_2 (Multiplicity of infection, 100). The medium was then removed and replaced with fresh medium. Cells stably overexpressing Foxc1 were then selected using puromycin incubation (2.5 μg/ml; cat. no. ST551; Beyotime Institute of Biotechnology) at 37˚C with 5% CO_2 for 7 days. Reverse transcription-quantitative PCR (RT-qPCR), western blotting and immunofluorescence analysis were used to detect transfection efficiency.

Small interfering RNA (siRNA) transfection. BV-2 cells were seeded in 6-well plates at a density of $5x10^4$ cells/ml for culturing at 37˚C with 5% CO_2 for 12 h before siRNA transfections (50 nM) were performed at ~80% confluency. IκBα expression in BV-2 cells was knocked down using siRNA (siRNA-IκBα sense, 5'-ACUCAUUGGUUCCUU UAAGGG-3' and antisense, 5'-CUUAAAGGAACCAAU GAGUCC-3'). A non-targeting siRNA (siRNA-NT) was used as a negative control (Santa Cruz Biotechnology, Inc.). Transfection of siRNAs into BV-2 cells was performed using the Lipofectamine® 3000 reagent (Invitrogen; Thermo Fisher Scientific, Inc.) at 37˚C with 5% CO_2 for 10 h. Transfection efficiency was measured using RT-qPCR and western blot analysis.

Animals. A total of 48 C57BL/6J mice, aged 8-10 weeks (weight, 25±5 g), were obtained from the Department of Experimental Animal Science, School of Medicine, Shanghai Jiao Tong University (license no. SYXK 2018-0027; Shanghai, China). All study procedures were approved by the Institutional Animal Care and Use Committee of Shanghai Jiao Tong University School of Medicine. All experimental procedures were conducted in accordance with the National Institutes of Health Guide for the Care and Use of Laboratory Animals (National Institutes of Health, revised in 1996) (28). Mice were housed in a temperature of 23±2˚C and humidity of 40-60% on a 12-h light-dark cycle with free access to food and water. Only male mice were used in the present study to minimize the risk of heterogeneity due to sex differences in the pathology of encephalopathy.

For the generation of Foxc1-overexpressing (Foxc1 OE) mice, embryonic stem (ES) cells (B6/BLU; cat. no. SCSP-226; The Cell Bank of Type Culture Collection of the Chinese Academy of Sciences) were cultured with the ES complete medium [600 ml, comprising DMEM (cat. no. 12430; Gibco;

Thermo Fisher Scientific, Inc.) 497 ml; fetal bovine serum (Gibco; Thermo Fisher Scientific, Inc.), 90 ml; Glutamax (cat. no. 35050-061; Gibco; Thermo Fisher Scientific, Inc.) 6 ml; MEM Non-Essential Amino Acids Solution (cat. no. 11140-050; Gibco; Thermo Fisher Scientific, Inc.), 6 ml; LIF (cat. no. ESG1107; MilliporeSigma), 60 μl (concentration, 1,000 U/ml), 2-Mercaptoethanol (cat. no. 21985023; Gibco; Thermo Fisher Scientific, Inc.) 1.5 ml] at 37˚C with 5% CO_2 and obtained from School of Medicine, Shanghai Jiao Tong University and transfected with the Foxc1 overexpression adenovirus (MOI, 100) for 72 h *in vitro*. The Foxc1-overexpressing ES cells were then transplanted into the uterus of female mice (10 male mice and 20 female mice were used in this study). In total, two litters of first-generation male and female mice were bred to obtain the Foxc1-overexpressing mice, where the Foxc1-overexpressing mice were reproduced indefinitely.

Experimental design. The sepsis mouse model was established using CLP surgery as described previously (29). Mice were randomly divided into the following four groups (n=12 per group): i) Naive; ii) sham operated; iii) CLP; and iv) CLP + Foxc1 overexpression (OE). A total of 6 days before and 10 days after CLP surgery, mice were subjected to the Morris water maze (MWM) trial for 6 days. The mice were then sacrificed after MWM trial, and the hippocampus tissues were removed for RT-qPCR and western blot analysis.

Mice with the following symptoms (humane endpoints) were be euthanized during the experiment: i) Inactivity or do not respond to gentle stimulation; ii) dyspnea, including signs of salivation and/or cyanosis from the nose and mouth; iii) diarrhea or urinary incontinence; iv) 20% weight loss; v) Inability to eat or drink; vi) clear signs of anxiety and irritability in animals; vii) paralysis, persistent epilepsy or rigid behavior and viii) infection and pus at the site of operation.

CLP surgery. For the CLP surgery itself (29), the mice were anesthetized using intraperitoneal injections of ketamine (80 mg/kg) and xylazine (5 mg/kg). After disinfection an incision was made below the xiphoid to expose the abdominal cavity. The cecum was then isolated, ligated and punctured twice using a 22-gauge needle. Intestinal contents were gently extruded into the peritoneal cavity. The abdomen was then sutured after the cecum was reinserted into the peritoneum. For the sham operated mice, the cecum was only exposed without ligation or perforation, before 1 ml sterile saline pre-warmed to 37˚C was put into the abdominal cavity. After surgery, mice were returned to their cages with a warm cotton pad and free access to food and water. Naive mice did not undergo laparotomy.

MWM trial. Spatial learning and memory were assessed using the MWM trial as described previously (30). Briefly, the water temperature was kept at 22-24˚C. Acquisition test was performed four times per day for 5 consecutive days; mice were put into the pool from four different directions and allowed to swim freely until they climbed up to platform under the water surface. If they did not find the platform within 60 sec, they were be guided to the platform and stayed on the platform for 10 sec. Four tests were conducted 20 min apart and their swimming track was recorded. The time of climbing to the hidden platform was defined as the escape latency. The platform was then removed on day 6 before retention tests were performed, mice were put into the pool from the same orientation and allowed to swim freely in the pool for 60 sec and the swimming track was recorded. The time of climbing to the hidden platform, the number of crossings over the platform area and the swimming speed were recorded. Experimental parameters were recorded using a SuperMaze Morris Water Maze video analysis system (model, XR-XM101; Shanghai XinRuan Information Technology Co., Ltd.).

Animal sample collection. From March to June 2021, mice were anesthetized using an intraperitoneal injection of 1% pentobarbital sodium (50 mg/kg). Mice were sacrificed by CO_2 inhalation using 30%/min volume displacement rate after cardiac saline perfusion, and the hippocampus tissues were then collected for subsequent experimentation.

RT-qPCR. RT-qPCR was performed as described previously (31). In brief, total RNA was extracted from BV-2 cells and hippocampal tissues using RNAiso Plus reagent (Takara Bio, Inc.), and then subjected to reverse transcription using a PrimeScript™ RT Master Mix kit (cat. no. RR036A; Takara Bio, Inc.) according to manufacturer's protocol. cDNA was used for qPCR with a TB Green® Premix Ex Taq™ (Tli RNaseH Plus) kit (cat. no. RR420A; Takara Bio, Inc.) according to the manufacturer's protocol. All procedures were performed in triplicate. The mRNA expression levels were calculated relative to the GAPDH using the the $2^{-\Delta\Delta Cq}$ method. The sequences of the primers used were as follows: Foxc1 forward, 5'-AAGACGGAGAACGGTACGTG-3' and reverse, 5'-TCACCGGGGAGTTGTTCAAG-3'; IκBα forward, 5'-TGTGCTTCGAGTGACTGACC-3' and reverse, 5'-TCACCCCACATCACTGAACG-3' and GAPDH forward, 5'-AGGTCGGTGTGAACGGATTTG-3' and reverse, 5'-TGTAGACCATGTAGTTGAGGTCA-3'. The full thermocycling conditions used for qPCR were as follows: Initial denaturation at 95˚C for 30 sec; followed by 40 cycles at 95˚C for 5 sec, 60˚C for 34 sec, 95˚C for 15 sec, 60˚C for 60 sec and 95˚C for 15 sec.

Western blot analysis. Western blot analysis was performed as described previously (32). The total protein content of cells and hippocampal samples was extracted using RIPA solution (cat. no. P0013B; Beyotime Institute of Biotechnology) for 30 min, and a BCA assay kit (cat. no. P0012S; Beyotime Institute of Biotechnology) was used to detect the total protein concentration. The extracted proteins (30 μg/lane) were separated by sodium dodecyl sulfate-polyacrylamide gel electrophoresis on 10% gels (Invitrogen; Thermo Fisher Scientific, Inc.) and were then transferred onto nitrocellulose membranes (MilliporeSigma), which were blocked with 5% non-fat milk at room temperature for 2 h, incubated with the corresponding primary at 4˚C overnight and secondary antibodies at room temperature for 2 h. The mouse antibodies used in the present study are listed: Foxc1 (1:1,000; cat. no. ab227977; Abcam), p65 (1:1,000; cat. no. ab32536; Abcam), IκBα (1:1,000; cat. no. ab32518; Abcam), allograft inflammatory factor 1 (Iba-1; 1:1,000; cat. no. ab178846; Abcam), IL-1β (1:1,000; cat. no. ab254360; Abcam), TNF-α (1:1,000; cat. no. ab215188;

Abcam), and β-actin (1:1,000; cat. no. ab179467; Abcam), HRP-conjugated goat anti-rabbit IgG H&L secondary antibody (1:2,000; cat. no. ab7090; Abcam). Protein bands were detected using an enhanced chemiluminescence reagent (cat. no. WBKLS0100; MilliporeSigma), visualized using a Bio-Rad ChemiDoc XRS imaging system (Bio-Rad Laboratories, Inc.) and analyzed by Image J software (version no: 1.51, National Institute of Health) and normalized to that of β-actin.

Cell proliferation assay. The viability of BV-2 cells was evaluated using the Cell Counting Kit-8 (CCK-8; MedChemExpress) assay in accordance with the manufacturer's protocol. Briefly, the BV-2 cells with or without Foxc1 overexpression were seeded into 96-well plates ($2x10^5$ cells/well) and cultured at 37˚C for 12 h. After treatment with or without LPS at 37˚C for 6 h, 10 ml CCK-8 solution was added into each well and cultured at 37˚C for 2 h, after which the optical density of each well was determined at 450 nm using a multiplate reader.

Transwell migration assay. The effect of Foxc1 on the migration of BV-2 cells was examined using Transwell chambers (pore size, 8-μm). Cells in different groups suspended in serum-free DMEM were seeded into the top chamber at a density of $3x10^5$ cells/well, whereas 500 μl complete DMEM containing 10% FBS was added to the lower chamber. The cells were allowed to migrate for 24 h at 37˚C in 5% CO_2. Cells on the upper surfaces of each chamber were removed using a cotton swab, before the chambers were fixed with 4% paraformaldehyde at room temperature for 30 min followed by 0.4% crystal violet staining at room temperature for 15 min. In total, five random fields of view were counted per chamber using an inverted microscope under a light field (x40 magnification; Olympus BX51; Olympus Corporation).

H&E staining. The hippocampal tissues were fixed with 4% paraformaldehyde at room temperature overnight, embedded in paraffin, sliced into 40-μm sections and dewaxed at 65˚C for 30 min. Sections were then incubated twice with xylene for 8 min and once for 5 min, followed by incubated three times with 100% alcohol for 5 min and once with 75% alcohol for 3 min, and rinsed with water for 5 min. Finally, slices were stained at room temperature with hematoxylin for 3 min and eosin for 25 sec, and were observed using an inverted microscope under a light field (x40 magnification; Olympus BX51; Olympus Corporation).

Immunofluorescence analysis. After tissue fixation, embedding, slicing and dewaxing as aforementioned, the antigen retrieval was performed using Improved Citrate Antigen Retrieval Solution (cat. no. P0083; Beyotime Institute of Biotechnology) at 95-100˚C for 20 min. Slices were then blocked with Immunol Staining Blocking Buffer (cat. no. P0102; Beyotime Institute of Biotechnology) at room temperature for 60 min, and were incubated with primary antibodies as follows: Iba-1 (1:100; cat. no. ab178846; Abcam) at 4˚C overnight.

Cells were fixed with 4% paraformaldehyde at room temperature for 15 min followed by permeabilization with 0.03% Triton X-100 and blocked with 5% BSA (cat. no. ST025; Beyotime Institute of Biotechnology) at room temperature for 30 min. They were then incubated with the Foxc1 antibody (1:100; cat. no. ab227977; Abcam) at 4˚C overnight in a humidified box. Antibodies were diluted using Immunol Staining Primary and secondary Antibody Dilution Buffer (cat. nos. P0103 and P0108; Beyotime Institute of Biotechnology).

On the following morning, the cells or tissue sections were washed with 1X TBST solution (cat. no. XY51287; Shanghai Xinyu Biotechnology Co., Ltd.) and incubated with Alexa Fluor® 647-conjugated goat anti-mouse IgG (1:100, cat. no. ab150115, Abcam) at room temperature for 1 h and labeled with DAPI (1 mg/ml; cat. no. 62247; Thermo Fisher Scientific, Inc.) at room temperature for 5 min. The fluorescence intensity was observed in three fields of view using fluorescence microscopy (x40 magnification; Olympus BX51; Olympus Corporation) and analyzed by ImageJ software.

TUNEL assay. Apoptosis was detected using the TUNEL Apoptosis Assay kit (cat. no. C1088; Beyotime Institute of Biotechnology). Briefly, after tissue fixation, embedding, slicing, dewaxing and antigen retrieval as aforementioned, 40-μm tissue sections were treated with 0.1% Triton X-100 for 10 min, and then incubated with TUNEL reagent at 37˚C in the dark for 60 min. The nuclei were stained with 5 μg/ml DAPI at room temperature for 5 min. The morphological changes of apoptotic cells were observed under a fluorescence microscope in three fields of view (Olympus BX51; Olympus Corporation). Green fluorescence was considered to indicate apoptotic cells.

ELISA. BV-2 cells with or with Foxc1 overexpression were seeded into 12-well plates ($5x10^5$ cells/well) and cultured at 37˚C for 12 hBV-2 cells were treated with or without LPS at 37˚C for 6 h. Finally, IL-1β and TNF-α in supernatants were measured by ELISA kits (cat. nos. 432601 and 430907; BioLegend, Inc.) following the manufacturers' protocols.

Flow cytometry analysis. HT-22 neuronal cells were purchased from The Cell Bank of Type Culture Collection of the Chinese Academy of Sciences to explore the effects of microglia-mediated inflammatory response on neuronal cells. HT-22 cells were routinely cultured in DMEM (Gibco; Thermo Fisher Scientific, Inc.) supplemented with 10% FBS (Gibco; Thermo Fisher Scientific, Inc.) and 2 mM L-glutamine, penicillin (100 U/ml) and streptomycin (100 g/ml; Gibco; Thermo Fisher Scientific, Inc.) at 37˚C with 5% CO_2. HT-22 cells ($1x10^5$ cells/ml) were cultured with the BV-2 cell-conditioned medium under different conditions at 37˚C with 5% CO_2 for 12 h. Suspended HT-22 cells were washed twice with PBS containing 2% FBS and stained with Annexin V FITC Apop Dtec Kit (cat. no. 556547; Becton-Dickinson and Company). In brief, 100 μl binding buffer before 5 μl FITC-labelled Annexin V (20 μg/ml) and 5 μl PI (50 μg/ml) were added and incubated in the dark at room temperature for 15 min. A tube without Annexin V FITC and PI was used as Blank, whereas Annexin V or PI was used the single-standard control. In total, 400 μl binding buffer was added at the end of the experiment and then assessed by flow cytometry (CytoFlex; Beckman Coulter, Inc.). The percentage of early- and late-stage

apoptotic cells was calculated using FlowJo v10 software (FlowJo, LLC).

Statistical analysis. The data are presented as the mean ± standard deviation from three independent experiments. Differences between/among groups were determined using an unpaired Student's t-test or one-way ANOVA followed by Tukey's post hoc test. A two-way ANOVA was performed for cell proliferation and a mixed ANOVA was used to analyze swimming speed and latency data from the MWM followed by Bonferroni correction for multiple testing. Statistical analyses were performed using the SPSS software (version 26.0; IBM Corp.). $P<0.05$ was considered to indicate a statistically significant difference.

Results

LPS triggers the inflammatory response in microglia and promotes neuronal apoptosis. After LPS treatment, the expression levels of Foxc1, p65 and IκBα of the NF-κB signaling pathway in microglial cells was measured by both RT-qPCR and western blot analysis. Foxc1 and IκBα expression was found to be significantly decreased, whereas that of p65 was significantly increased compared with that in the control group (Fig. 1A-E). In addition, the secretion of IL-1β and TNF-α (Fig. 1F) by BV-2 cells was next examined using ELISA, where the results showed that LPS significantly increased the secretion of IL-1β and TNF-α compared with that in the control group. Subsequently, HT-22 neurons were cultured with the media conditioned by BV-2 cells in the control or LPS-treated groups, respectively. The percentage of neuronal apoptosis was then measured by flow cytometry, which showed that the levels of HT-22 cell apoptosis in the LPS-treated BV-2 media group were significantly higher compared with those in the control group (Fig. 1G and H). These results suggest that microglia-mediated inflammatory response induced by LPS resulted in neuronal apoptosis.

Overexpression of Foxc1 inhibits microglia-mediated inflammatory response and neuronal apoptosis induced by LPS. After adenoviral transfection, the expression of Foxc1 in BV-2 cells with or without LPS treatment was significantly increased compared with that in the Ad-Ctrl group, according to western blotting (Fig. 2A, B, D and E), RT-qPCR (Fig. 2C) and immunofluorescence analysis observations (Fig. 2F and G). Subsequently, the expression of p65 and IκBα was measured using western blot analysis, whereas the secretion of IL-1β and TNF-α by BV-2 cells was examined by ELISA. Foxc1 overexpression significantly reduced the expression of p65 whilst upregulating the expression of IκBα compared with those in the Ad-Ctrl group in the presence of LPS (Fig. 2H and I). The secretion of IL-1β and TNF-α by BV-2 cells also exhibited a similar trend as p65, in that significant reversals of the LPS-induced upregulation in secretion were observed (Fig. 2J). HT-22 neurons were next cultured with the media conditioned by BV-2 cells in the control, Ad-Ctrl and Ad-Foxc1 groups with LPS treatment. The extent of neuronal apoptosis in the Ad-Foxc1 group was significantly lower compared with that in the Ad-Ctrl group (Fig. 2K and L). These results suggest that overexpression of Foxc1 inhibited LPS-induced inflammatory responses and neuronal apoptosis by deactivating of NF-κB signaling.

Overexpression of Foxc1 inhibits LPS-induced microglial migration, inflammation and neuronal apoptosis through the inhibition of IκBα/NF-κB signaling. To investigate the underlying regulatory mechanism of Foxc1 on the inflammatory response, microglial migration and neuronal apoptosis induced by LPS, the effect of Foxc1 overexpression on microglial migration, NF-κB signaling and neuronal apoptosis was next investigated. Transwell assay revealed that LPS markedly increased microglial migration compared with that in the blank group (BV-2 cells without any treatment). Foxc1 overexpression significantly inhibited microglial migration compared with that in the Ad-Ctrl group in the presence of LPS (Fig. 3A and B). Subsequently, the effect of Foxc1 overexpression and LPS treatment on the viability of BV-2 cells was also evaluated using CCK-8 assay, which showed that neither Foxc1 overexpression nor LPS treatment could influence the viability of BV-2 cells (Fig. 3C and D). These results suggest that Foxc1 overexpression inhibited microglial migration induced by LPS without affecting viability. Subsequently, to determine the effect of Foxc1 overexpression on NF-κB signaling during the LPS-induced inflammatory response, the expression of IκBα in Foxc1-overexpressing BV-2 cells was knocked down using siRNA-IκBα in the absence or in the presence of LPS. Both western blot analysis and RT-qPCR results showed that the expression of IκBα in the siRNA-IκBα group was significantly decreased compared with that in the siRNA-NT (the negative silenced) group, though no significant difference could be found between the siRNA-NT and control groups (Fig. 3E-I). In addition, the expression of p65 in the siRNA-IκBα group was significantly increased compared with that in siRNA-NT group, but no significant difference could be found between the siRNA-NT and the control groups (Fig. 3H and I). Transwell assay results demonstrated that knocking down IκBα expression significantly promoted microglial migration compared with that in the siRNA-NT group (Fig. 3J and K). ELISA results revealed that the secretion of IL-1β and TNF-α by BV-2 cells were significantly increased in the siRNA-IκBα group compared with that in the siRNA-NT group (Fig. 3L). Subsequently, HT-22 neurons were cultured with the media conditioned by BV-2 cells in the control, siRNA-NT and siRNA-IκBα groups in Foxc1-overexpressing BV-2 cells treated with LPS. HT-22 cell apoptosis in siRNA-IκBα group was found to be significantly increased compared with that in siRNA-NT group, but no statistical significance was found between the siRNA-NT and control groups (Fig. 3M and N). These data suggest that Foxc1 overexpression attenuated LPS-induced inflammatory response, microglial migration and neuronal apoptosis by inhibiting IκBα/NF-κB pathway.

Cognitive impairments and downregulation of Foxc1/IκBα in sepsis-associated encephalopathy. Establishment of the mouse septic encephalopathy model by CLP, animal behavior and molecular experiments were performed as shown in Fig. 4A. Before CLP surgery, mouse cognitive ability, including learning, memory, and spatial orientation, were evaluated using the MWM test. Results showed that the learning and memory abilities of spatial orientation were not significantly different among the four groups (Fig. S1), suggesting that Foxc1 overexpression did not alter the cognitive ability of the mice. After CLP surgery, MWM test results showed that the

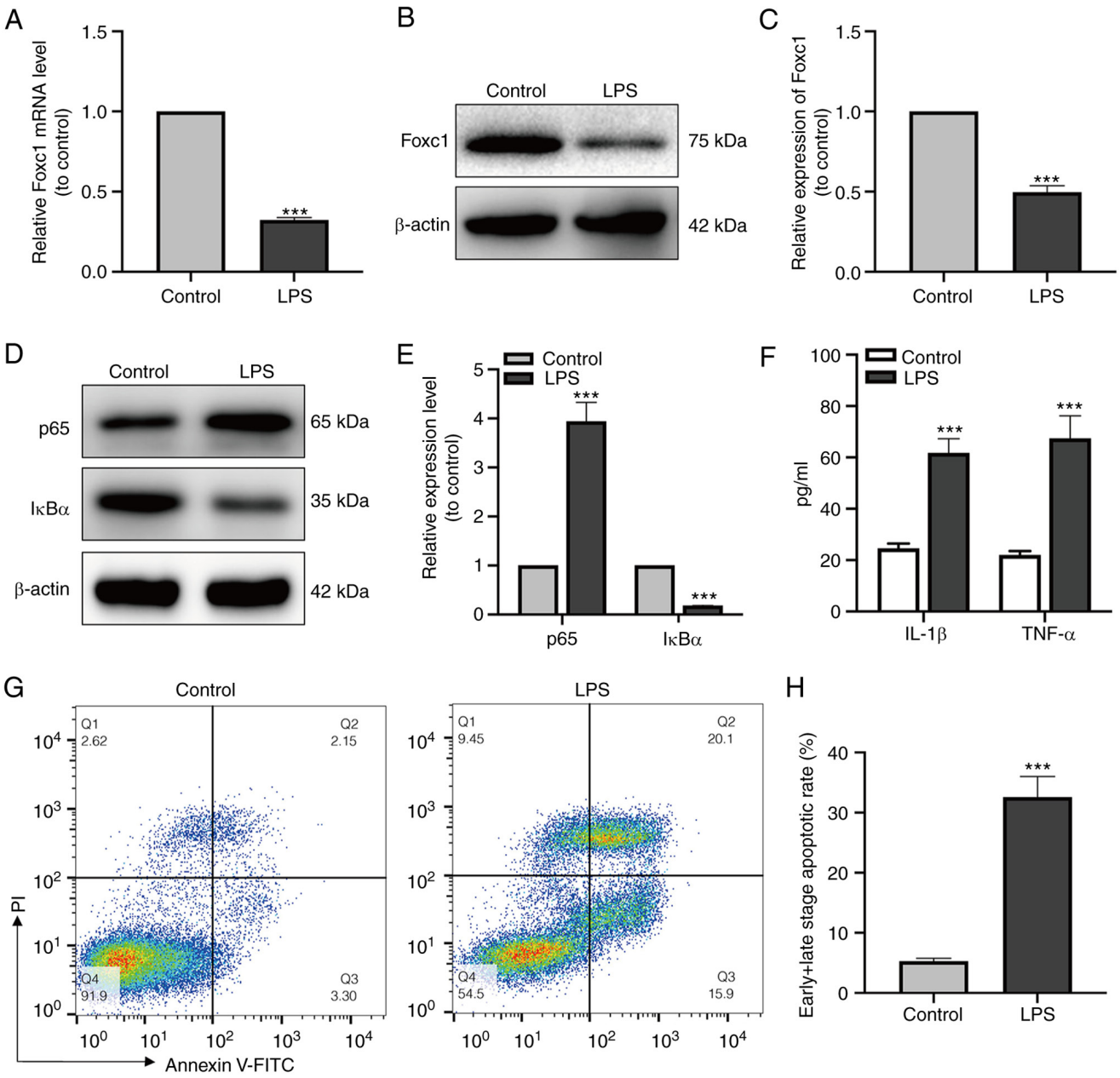

Figure 1. LPS triggers the inflammatory response in BV-2 cells and induce HT-22 cell apoptosis. (A) Reverse transcription-quantitative PCR and (B) western blot analysis were used to detect differences in the expression of Foxc1 expression between the control and LPS groups. (C) Quantification of western blotting data shown in (B and D) p65 and IκBα expression in the control and LPS groups were measured using western blot analysis, (E) which were quantified. (F) IL-1β and TNF-α secretion into the cell culture supernatant by BV-2 cells in control and LPS groups were detected by ELISA. (G) Flow cytometry analysis of HT-22 neuronal apoptosis after incubation in the media conditioned by microglia; the percentage of early and late apoptotic cells was measured by flow cytometry and (H) early + late apoptotic rate was quantified. Data represents the mean ± SD from three independent experiments. ***P<0.001 vs. Control. LPS, lipopolysaccharide; Foxc1, Forkhead box C1; IκBα, NF-κB inhibitor α.

swimming speed exhibited no statistical difference throughout the 6 consecutive days (Fig. 4B), suggesting that neither Foxc1 overexpression nor CLP surgery affected the motor ability of the mice. However, mice in the CLP surgery group exhibited significantly longer escape latency compared with that in the sham-operated group (Fig. 4C). Dwell time in the target quadrant and the frequency of passing through the target platform area were also significantly reduced in the CLP surgery group compared with those in the sham-operated group (Fig. 4D and E). The escape latency of mice in the Foxc1 overexpression group was significantly shorter compared with that in CLP group, whereas the dwell time in the target quadrant and the frequency of passing through the target platform area were significantly increased in the Foxc1 overexpression group compared with those in the CLP group (Fig. 4C and E). This suggests that CLP surgery impaired the cognitive ability of the mice, which was partially prevented by Foxc1 overexpression. Subsequently, the mRNA expression levels of Foxc1 and IκBα in the hippocampus tissues of the mice on days 3, 7 and 14 after CLP surgery were measured by RT-qPCR, which showed that the expression levels of Foxc1 (Fig. 4F) and IκBα (Fig. 4G) were significantly reduced compared with those in the sham-operated group on days 3, 7 and 14 after CLP surgery. These *in vivo* results suggest that CLP resulted

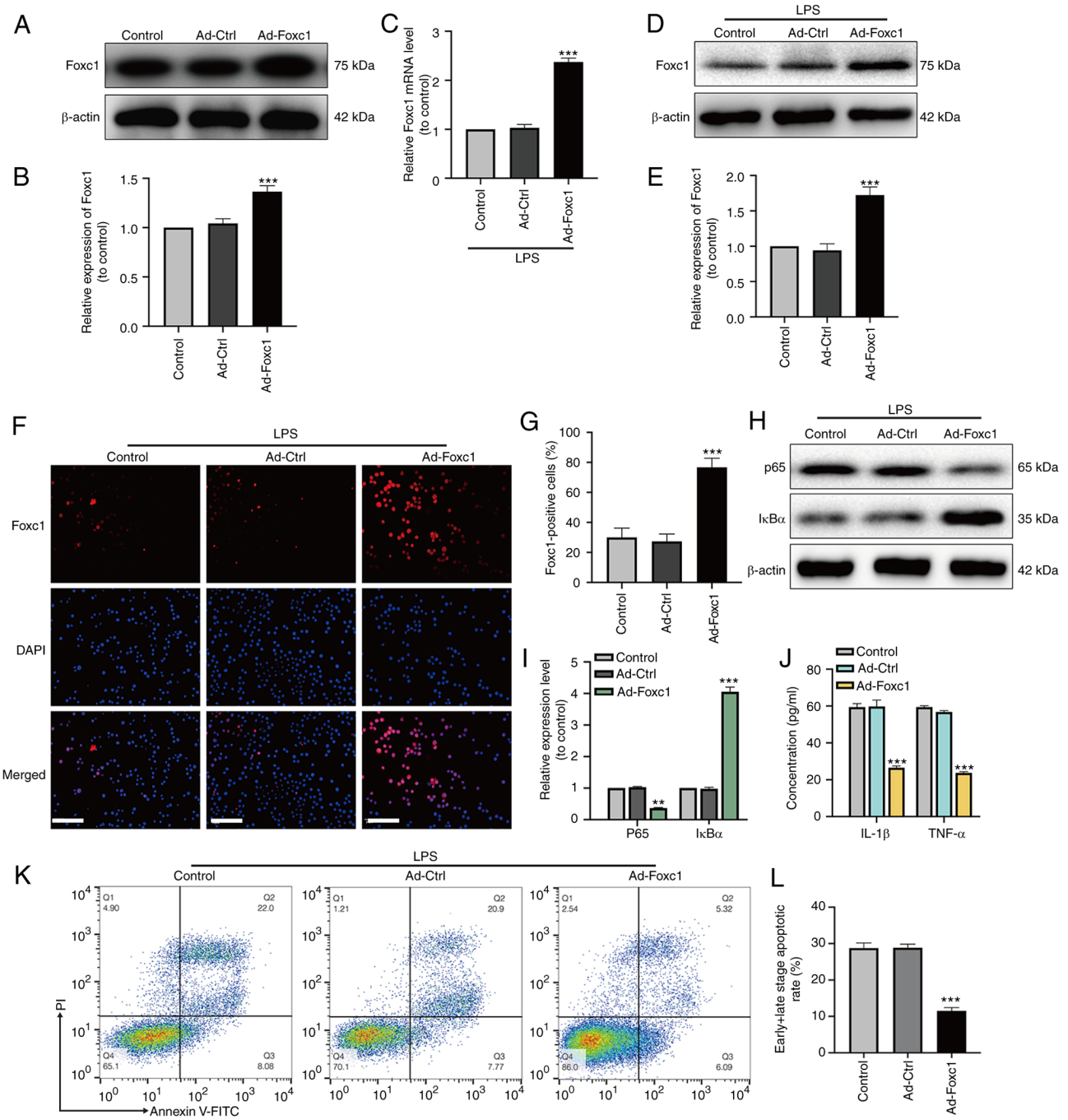

Figure 2. Overexpression of Foxc1 inhibits microglia-mediated inflammatory response and neuronal apoptosis induced by LPS. After adenoviral transfection, transfection efficiency was analyzed by (A) western blot analysis and (B) was semi-quantified. After LPS treatment, the expression of Foxc1 was analyzed by (C) reverse transcription-quantitative PCR and (D) western blot analysis, (E) the latter of which was quantified. (F) Immunofluorescence assay was performed to detect Foxc1 overexpression in BV-2 cells following LPS-treatment. Untreated BV-2 cells were used as the control group. Scale bar, 20 μm. (G) Percentage of Foxc1-positive BV-2 cells. (H) In the presence of LPS, the expression levels of p65 and IκBα in BV-2 cells in the three groups were detected by western blot analysis and (I) quantified. (J) In the presence of LPS, the secretion of IL-1β and TNF-α into the culture supernatant by BV-2 cells in the three groups were detected by ELISA. (K) Flow cytometry analysis of HT-22 cell apoptosis after incubation in the media conditioned by microglia. (L) The percentage of early and late apoptotic HT-22 cells was examined by flow cytometry analysis. Data represents the mean ± SD of three independent experiments. **P<0.01 and ***P<0.001 vs. Ad-Ctrl group. LPS, lipopolysaccharide; Ad-, adenovirus; Ctrl, control; Foxc1, Forkhead box C1; IκBα, NF-κB inhibitor α.

in cognitive impairment in addition to the downregulation of Foxc1 and IκBα expression in the hippocampus of the mice. Consequently, Foxc1 and IκBα may regulate the cognitive function of mice during inflammation.

NF-κB signaling is involved in mediating the hippocampal inflammatory response and microglial migration in mice with SAE. After CLP surgery, to verify the establishment of SAE, MWM trial and H&E staining were performed. Mice in the group showed significantly longer latency and shorter dwell times in the goal quadrant compared with those in the sham-operated group (Fig. 4C-E). H&E staining demonstrated that in the CLP group, the hippocampal structure was disordered, where the nuclei of neurons were condensed and the

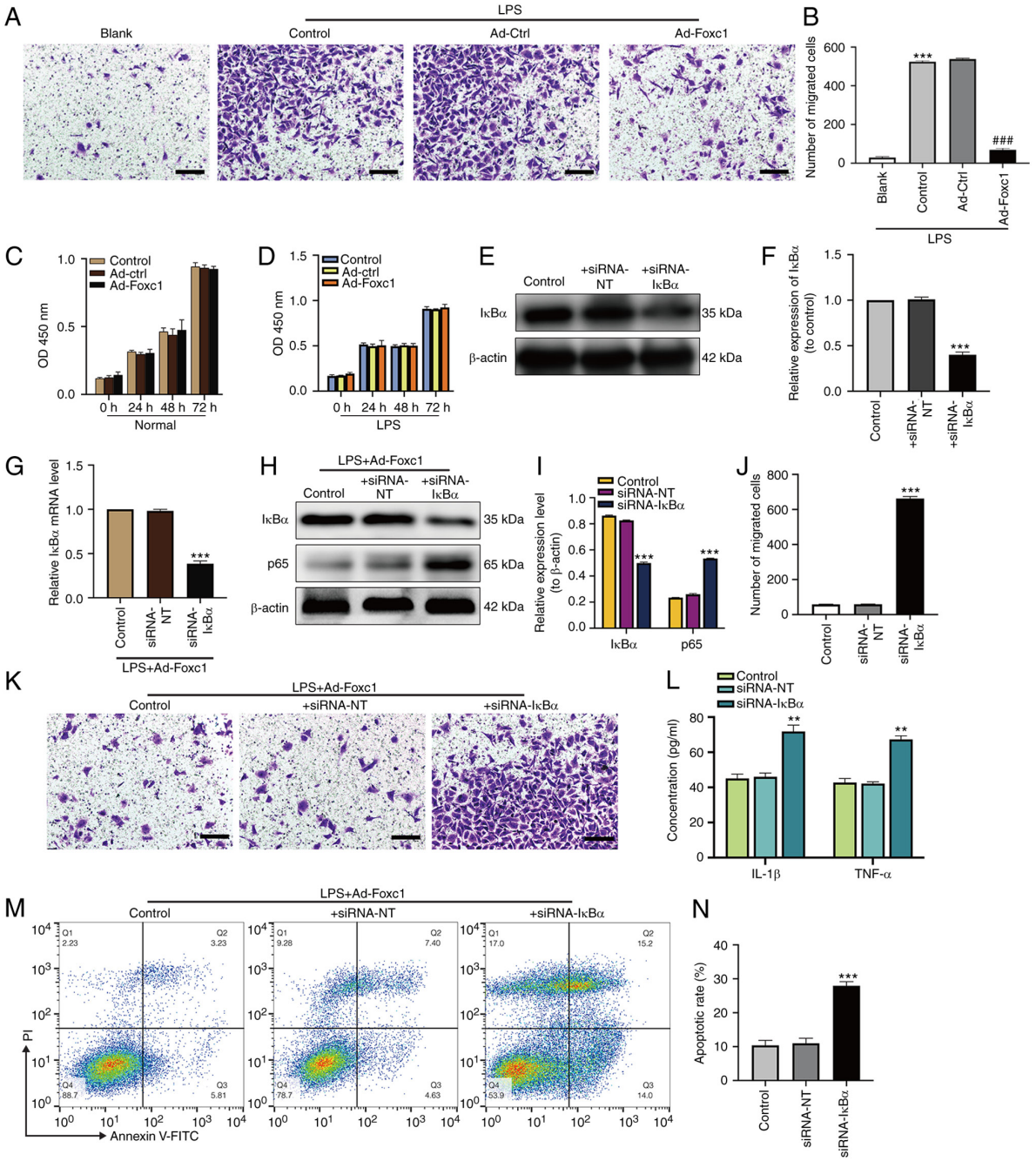

Figure 3. Overexpression of Foxc1 inhibits LPS-induced microglial migration, inflammatory response and neuronal apoptosis through the NF-κB pathway. (A) Representative images showing migrated BV-2 microglial cells with or without Foxc1 overexpression under normal or LPS conditions using Transwell assays, (B) which were quantified. Scale bar, 50 μm. ***P<0.001 vs. blank group; $^{###}$P<0.001 vs. Ad-Ctrl group. Viability of BV-2 cells under (C) normal or (D) LPS conditions with or without Foxc1 overexpression were determined by the CCK-8 assay. After siRNA transfection, transfection efficiency was analyzed by (E) western blot analysis and (F) was semi-quantified. In the presence of LPS, BV-2 cells with Foxc1 overexpression were transfected with siRNA-IκBα or with siRNA-NT. Foxc1-overexpressing BV-2 cells without siRNA transfection were used as the control group. siRNA-mediated transfection efficiency on IκBα and p65 expression was determined by (G) reverse transcription-quantitative PCR and (H) western blot analysis, (I) the latter of which was quantified. (H) Quantification of BV-2 cell migration after Foxc1 overexpression in the presence of LPS using Transwell assays. (J) Representative Transwell assay images, (K) which were quantified. Scale bar, 50 μm. (L) After siRNA transfection, the secretion of IL-1β and TNF-α into the cell culture supernatant by BV-2 cells with Foxc1 overexpression in the presence of LPS was measured by ELISA. (M) Flow cytometry analysis of HT-22 cell apoptosis after incubation in the media conditioned by microglia. (N) The percentage of early and late apoptotic HT-22 cells was measured by flow cytometry analysis. Data represents the mean ± SD of three independent experiments. **P<0.01 and ***P<0.001 vs. + siRNA-NT group. LPS, lipopolysacharide; Ad-, adenovirus; Ctrl, control; siRNA, small interfering RNA; Foxc1, Forkhead box C1; IκBα, NF-κB inhibitor α.

cytoplasm were swollen (Fig. 5A). The expression of Foxc1 and IκBα in hippocampal tissue of mice were measured by western blot analysis. The expression of Foxc1 and IκBα were significantly reduced in the CLP group compared with that in the Sham group (Fig. 5B and C). Additionally, the expression of p65, a subunit in NF-κB family and Iba-1, a microglia marker, were detected by western blot analysis. The expression of both p65 and Iba-1 in the hippocampal tissues of mice were found to be significantly increased in the CLP group compared with that in the Sham group (Fig. 5D and E). Subsequent

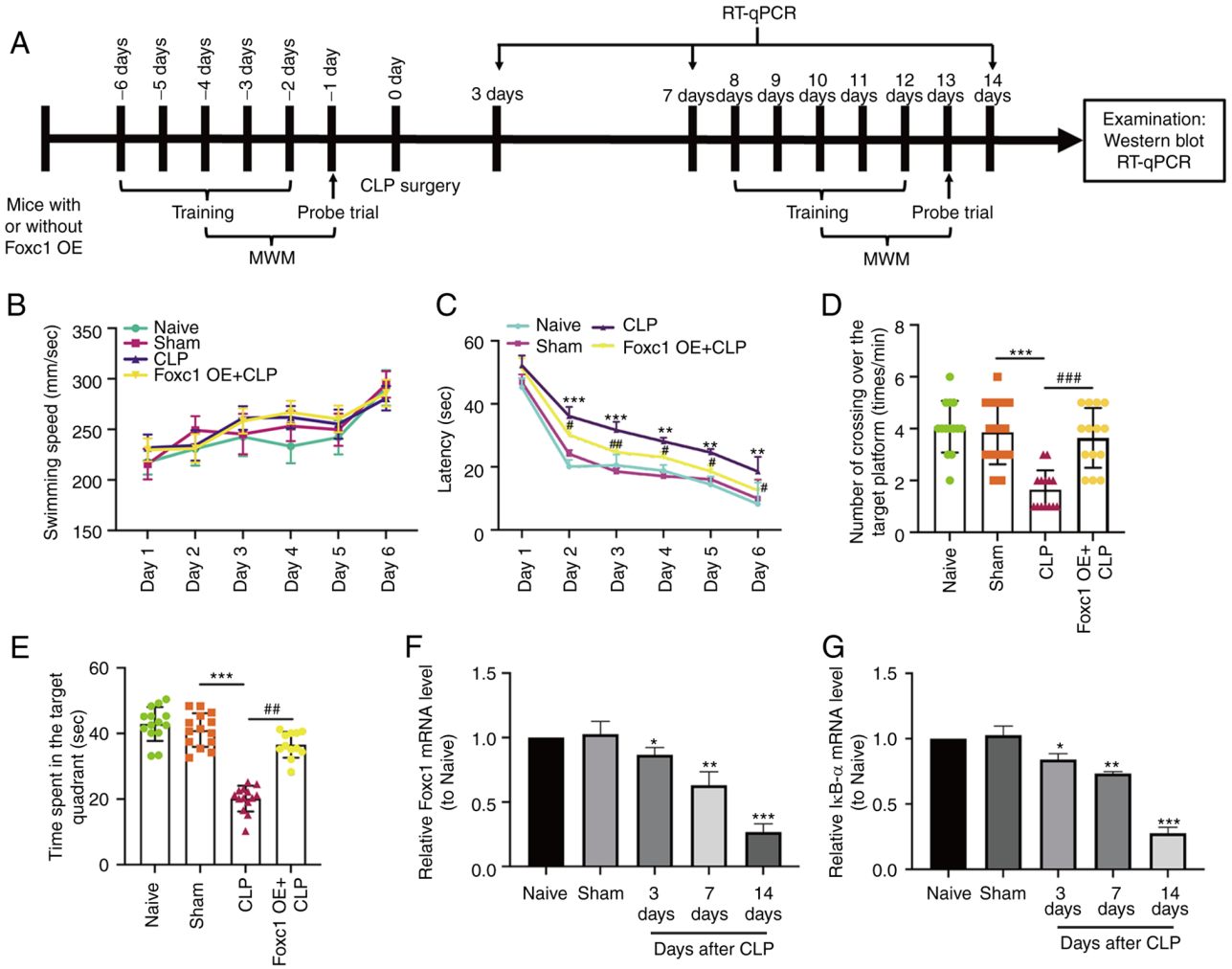

Figure 4. Cognitive impairment and downregulation of Foxc1 and IκBα expression in sepsis-associated encephalopathy. (A) Timeline of the Morris Water Maze (MWM) protocol, RT-qPCR and western blotting in naive, sham-operated, CLP-operated and CLP + Foxc1 OE mice. (B-E) Cognitive function of mice in each treatment group was analyzed by MWM test. (B) Average swimming speed throughout the 6 consecutive days among the four experimental groups. (C) Latency, defined as the time the mouse took to find the hidden platform or first passed through the area where the platform was located. (D) The frequency of passing through the area where the platform was located was recorded. (E) Dwell time in the quadrant where the platform was located. n=14. The mRNA expression of (F) Foxc1 and (G) IκBα in the hippocampus tissues of mice with or without CLP surgery were detected by RT-qPCR. Data represents the mean ± SD of three independent experiments. *P<0.05, **P<0.01 and ***P<0.001 vs. Sham. $^{\#}$P<0.05, $^{\#\#}$P<0.01 and $^{\#\#\#}$P<0.001 vs. CLP group. CLP, cecal ligation and perforation; OE, overexpression; MWM, Morris Water Maze; Foxc1, Forkhead box C1; IκBα, NF-κB inhibitor α.

western blot analysis of IL-1β and TNF-α expression in the hippocampal tissues also showed that the expression both of these cytokines were significantly increased in the CLP group compared with that in the Sham group (Fig. 5F and G). These data suggest that NF-κB pathway may serve important roles in the hippocampal inflammatory response and microglial migration during SAE.

Overexpression of Foxc1 attenuates cognitive dysfunction by inhibiting microglial migration, inflammation and neuronal apoptosis in the hippocampus of mice with SAE through the IκBα/NF-κB pathway. The expression of Foxc1 in the hippocampus of mice with or without Foxc1 overexpression before CLP surgery was assessed by western blot analysis, which revealed the success of Foxc1 overexpression in the hippocampus of mice (Fig. 6A and B). After CLP surgery, H&E staining demonstrated that the hippocampal structure appeared to be more ordered with cell volume smaller, where the extent of cytosolic edema was decreased in tissues from the Foxc1 overexpression group compared with those in the CLP group (Fig. 6C). To investigate the role of the NF-κB pathway in the hippocampal inflammatory response, microglial migration and neuronal apoptosis in mice with SAE, Foxc1-overexpressing mice were used. After CLP surgery, the expression of Foxc1 and IκBα in the hippocampus of mice were examined using western blot analysis. Results showed that the expression levels of Foxc1 and IκBα were significantly higher in the CLP + Foxc1 OE group compared with that in the CLP group (Fig. 6D and E). The effect of Foxc1 overexpression on the expression of p65, Iba-1, IL-1β and TNF-α in the hippocampus tissues of mice were next detected by western blot analysis, which showed that Foxc1 overexpression significantly inhibited the expression of p65, Iba-1, IL-1β and TNF-α in the compared with that in the CLP group (Fig. 6F-I). Subsequently, microglial migration and neuronal apoptosis in the hippocampus of mice were measured using immunofluorescence and TUNEL staining. The number of Iba-1-positive and TUNEL-positive cells were both marked increased in

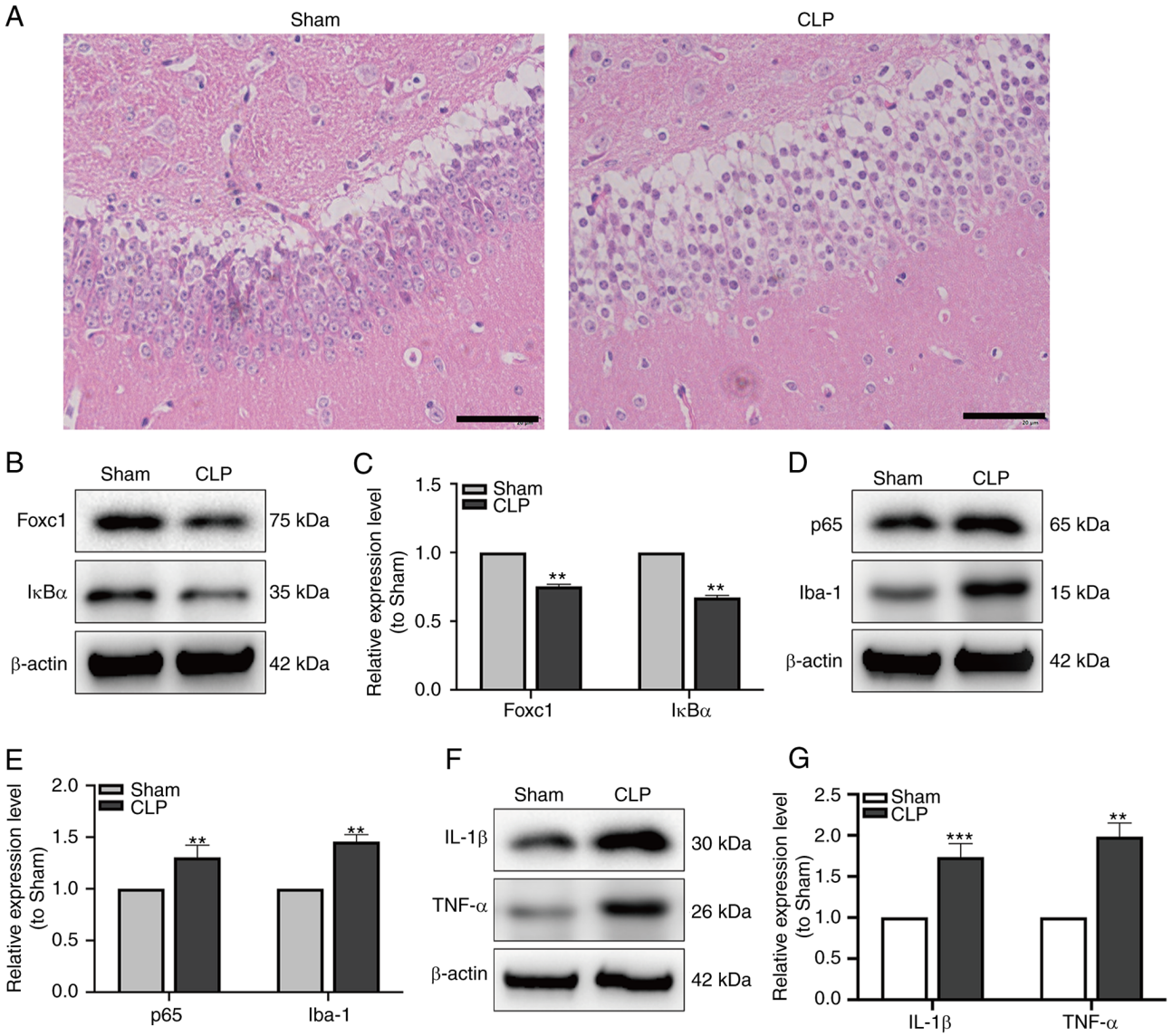

Figure 5. NF-κB pathway is involved in the hippocampal inflammatory response and microglial migration in mice with sepsis-associated encephalopathy. (A) H&E staining of the mouse hippocampal tissue. Scale bar, 20 μm. (B) The expression of Foxc1 and IκBα was measured by western blotting (C) and quantified. (D) The expression of p65 and Iba-1 was measured by western blotting (E) and quantified. (F) The expression of IL-1β and TNF-α was measured by western blotting (G) and quantified. Data represents the mean ± SD of three independent experiments. **P<0.01 and ***P<0.001 vs. Sham. Foxc1, Forkhead box C1; IκBα, NF-κB inhibitor α; CLP, cecal ligation and perforation; Iba-1, allograft inflammatory factor 1.

the CLP group compared with those in the Sham group, but the number of Iba-1-positive and TUNEL-positive cells in the CLP + Foxc1 OE group were both markedly decreased compared with those in the CLP group (Fig. 6J-L). These results suggest that Foxc1 overexpression can inhibit microglial migration, inflammation and neuronal apoptosis in the hippocampus of mice with SAE through the NF-κB pathway.

Discussion

The present study provided information on the potential mechanism underlying cognitive dysfunction in SAE. LPS induced inflammatory responses in the microglia, increased microglial migration and neuronal apoptosis in addition to downregulating Foxc1 and IκBα expression *in vitro*. Furthermore, sepsis induced by CLP surgery led to cognitive dysfunctions accompanied with increased longer escape latency, decreased dwell time in the target quadrant and decreased frequency of passing through the target platform area in the MWM test. Decreased expression of Foxc1 and IκBα, increased expression of p65, Iba-1, IL-1β and TNF-α and increased neuronal apoptosis were also observed in the hippocampal tissues of mice following CLP. It was found that Foxc1 overexpression promoted IκBα expression, inhibited microglial migration, inflammation and neuronal apoptosis both *in vitro* and *in vivo*, which prevented cognitive dysfunction in mice induced by CLP. In addition, IκBα knockdown using siRNA in microglial cells reversed the inhibitory effects of Foxc1 overexpression on the inflammatory response, microglial migration and neuronal apoptosis. Collectively, these data suggest that Foxc1 overexpression can inhibit microglial migration, hippocampal inflammatory response and neuronal apoptosis to alleviate sepsis-induced cognitive dysfunction.

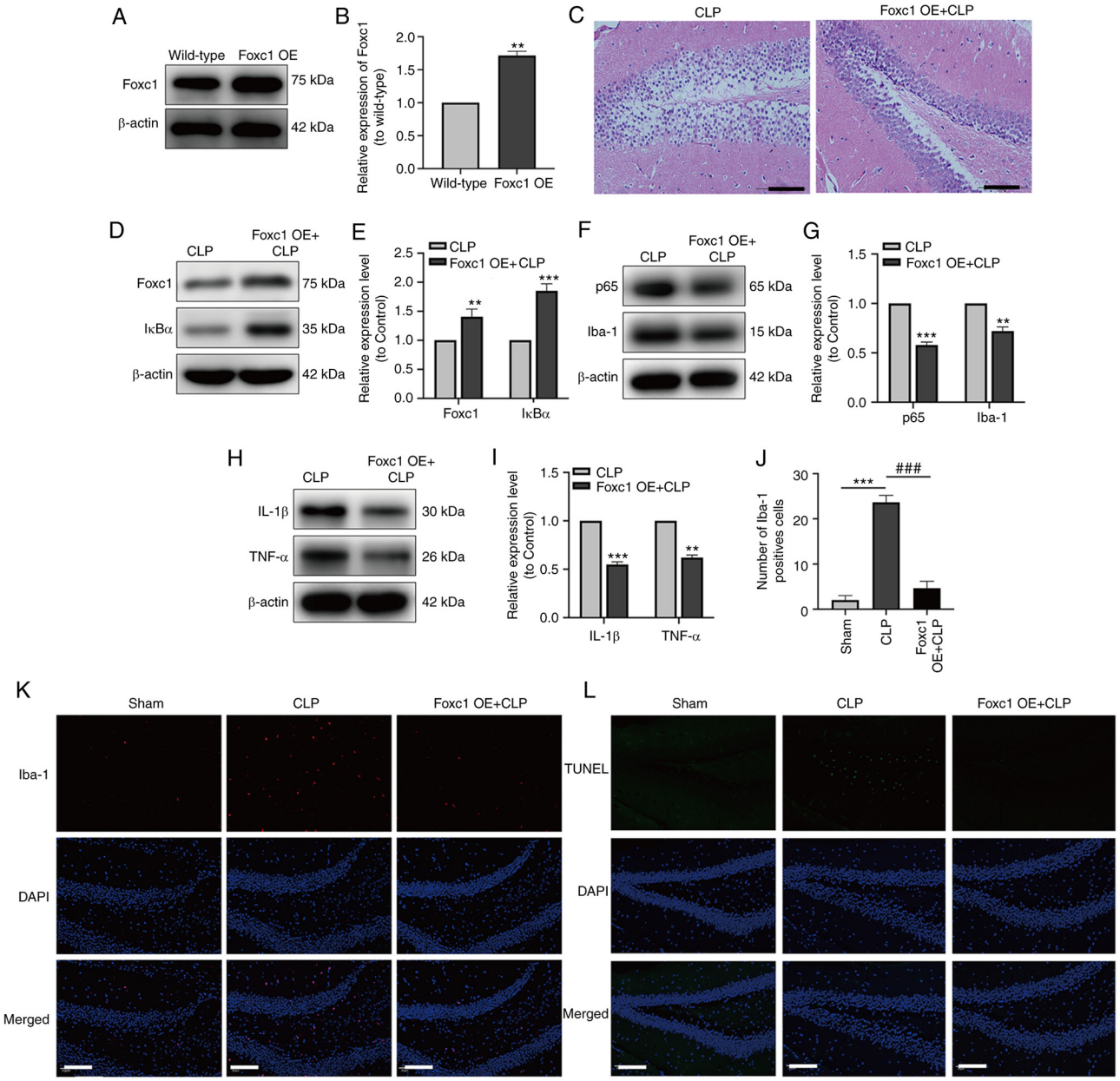

Figure 6. Overexpression of Foxc1 inhibits microglial migration, suppresses the inflammatory response and neuronal apoptosis in the hippocampus of mice with sepsis-associated encephalopathy through the NF-κB pathway. The expression of Foxc1 in the hippocampus of mice with or without Foxc1 overexpression was analyzed by (A) western blot analysis and (B) was semi-quantified, **P<0.01 vs. wild-type group. (C) H&E staining of the mouse hippocampal tissue. Scale bar, 100 μm. (D) The expression of Foxc1 and IκBα in hippocampal tissue of mice was measured by western blotting (E) and quantified. (F) The expression of p65 and Iba-1 in the hippocampal tissues of the mice was measured by western blotting (G) and quantified. (H) The expression of IL-1β and TNF-α in the hippocampal tissues of mice was measured by western blot analysis (I) and quantified. (K) Immunofluorescence staining quantification of Iba-1 in the mouse hippocampal tissue. (J) Representative immunofluorescence images of Iba-1 staining, where red dots represent microglia. Scale bar, 20 μm; n=3/group. (L) TUNEL staining, where green dots represent apoptotic neurons. Scale bar, 20 μm. **P<0.01 and ***P<0.001 vs. CLP or as indicated; $^{\#\#\#}$P<0.001 as indicated. Foxc1, Forkhead box C1; OE, overexpression; IκBα, NF-κB inhibitor α; CLP, cecal ligation and perforation; Iba-1, allograft inflammatory factor 1.

In the present study, LPS reduced the expression of Foxc1 in microglial BV-2 cells, whilst CLP surgery also downregulated the expression of Foxc1 in the hippocampus of mice compared with their corresponding control groups. Foxc1 contains a common 100-amino acid winged-helix DNA-binding domain that serves key roles in cell proliferation, differentiation migration and survival (19,33). A previous study showed that Foxc1 promoted the migration of hepatocellular carcinoma (HCC) cells, as knockdown of Foxc1 inhibited the migration of HCC cells (34). Additionally, overexpression of Foxc1 in breast cancer cells was found to increase proliferation, migration and invasion, whilst Foxc1 knockdown exerted opposite effects (22). The present study revealed that the overexpression of Foxc1 inhibited the LPS-induced microglial migration both *in vitro* and *in vivo*. This finding is not consistent with the previously reported effects of Foxc1 on cancer cellular migration.

Microglia is a highly specialized resident population of macrophage-like immune cells in the CNS that serves ambiguous functions, since they can mediate both neuroprotective and neurotoxic effects (35). Microglial cells serve essential roles in brain development and are responsible

for maintaining homeostasis in the CNS (36). In addition, microglia-mediated neuroinflammation serves important roles in neuronal repair and the regulation of inflammation in the CNS (37,38). However, microglia have also been shown to promote neuroinflammation-associated cognitive impairment (39). Activated microglia can polarize towards the M_1 and M_2 phenotypes (40). The M_1 phenotype mainly migrates towards the site of neuroinflammation, where it secretes a number of proinflammatory cytokines, including IL-1β, TNF-α and adhesion molecules (such as CD86) (40). These cytokines then disrupt the BBB, which potentiates further microglia activation, leading to a vicious cycle and eventual neuronal damage (41-43). By contrast, the M_2 phenotype is generally associated with tissue regeneration by secreting anti-inflammatory cytokines to inhibit microglia polarization into the M_1 phenotype (44,45). In the present study, LPS induced the secretion of IL-1β and TNF-α by the microglial cells, suggesting that LPS induced microglial polarization into the M_1 phenotype. In addition, increased IL-1β and TNF-α expression was observed in the hippocampal tissues of mice following CLP surgery. This is consistent with the findings from a previous hypoxic-ischemic brain injury study, which found that hypoxia-ischemia facilitated M_1 phenotype polarization whilst attenuating M_2 phenotype activation (46). It is noteworthy that the overexpression of Foxc1 decreased the expression of IL-1β and TNF-α in the present study, suggesting that Foxc1 overexpression promoted microglial polarization into the M_2 phenotype whilst suppressing the M_1 phenotype. Under physiological conditions, microglial cells are sparsely distributed in the CNS. After the CNS becomes infected or damaged, microglia will rapidly proliferate and migrate to the damaged site (47). In the present study, LPS was found to induce microglial migration *in vitro*, whereas the expression of Iba-1, a microglia marker protein, was also significantly increased in the hippocampal tissues of mice following CLP surgery. In addition, increased neuroinflammation was accompanied with increased microglial migration, suggesting that microglial migration promoted the inflammatory response. Given its key role in mediating neuroinflammation, the regulation of migration and phenotype polarization in microglia is likely to be an important factor in SAE. However, the regulatory mechanism remains unclear at present.

The NF-κB signaling pathway serves an important role in the regulation of inflammation; NF-κB normally exists in the cytosol as an inactive form, where it forms a complex with inhibitory IκBα proteins (48,49). NF-κB pathway has been previously reported to be part of the mechanism underlying SAE-related CNS damage (50). Members of the NF-κB family include p50, p52, p65, RelB and c-Rel subunits. In total, two separate activation pathways for NF-κB have been reported, namely the canonical pathway and the alternative pathway (51). In the canonical pathway, phosphorylated IκBα is degraded by the proteasome, causing it to separate from the IκBα/p65 complex (51). The p65 subunit is then released, where it translocates into the nucleus to promote NF-κB-dependent gene transcription (51). This results in the accumulation of NF-κB homodimers and heterodimers in the nucleus (51). Therefore, decreased expression of IκBα can be applied to indirectly measure the status of NF-κB activation (48). The alternative pathway can be activated by a small subset of tumor necrosis factors, such as CD40 ligand and lymphotoxin B. By contrast, the canonical pathway can also be activated by proinflammatory cytokines, such as TNF-α and IL-1, usually leading to the activation of NF-κB pathway; briefly, mitogen kinase and phosphorylated-IκBα protein kinase are activated, leading to the degradation of NF-κB p100 via phosphorylation, and the formation of the P52/RelB heterodimer and NF-κB P50/RelB heterodimer, which enter the nucleus and regulate the transcription of target genes (48). A previous study has reported that inflammatory encephalopathy enhanced NF-κB activity primarily through the canonical pathway (52). The present study showed that LPS treatment downregulated the expression of IκBα but upregulated the expression of p65 in microglia, suggesting that the activation of NF-κB was likely through the canonical pathway. This notion was supported further by observations of increased IL-1β and TNF-α secretion/expression. However, the underlying mechanism of this LPS-induced activation of NF-κB pathway in microglia require further study.

To examine the association between Foxc1 and IκBα in SAE-related hippocampal inflammatory response, the expression of Foxc1 was overexpressed in microglia. Overexpression of Foxc1 was found to upregulate the expression of IκBα in microglia, in addition to inhibiting microglial migration and the inflammatory response, suggesting that overexpression of Foxc1 stabilized the IκBα/p65 complex and inhibited p65 activation to suppress the transcription of proinflammatory cytokines in microglia. Subsequently, the expression of IκBα was then knocked down in microglia, which reversed the inhibitory effects of Foxc1 overexpression on microglial migration and inflammation. This suggests that Foxc1 overexpression inhibits the NF-κB pathway by promoting the expression of IκBα, which then inhibits microglial migration and inflammation during SAE. Microglia-mediated neuroinflammatory response has been reported to at least partially mediate the pathology of various neurodegenerative diseases, including Alzheimer's disease, Parkinson's disease (PD) and multiple sclerosis (53-55). A number of studies have documented that microglia-mediated inflammation can aggravate neuronal axon and synaptic damage, increase demyelination, destroy the integrity of the white matter and induce neuronal apoptosis, all of which eventually leading to progressive neurodegeneration or even death (40,56,57). The present study also showed that mice following CLP surgery manifested cognitive impairments accompanied with increased neuroinflammation and neuronal apoptosis in the hippocampus, in accordance with the hypothesis that neuroinflammation is deleterious to CNS. In addition, overexpression of Foxc1 was found to inhibit neuroinflammation, neuronal apoptosis whilst alleviating cognitive dysfunction in the present study, this suggests that the anti-inflammatory function of Foxc1 may contribute to protective effects against sepsis-induced neuronal impairments and cognitive dysfunction.

In conclusion, *in vitro* and *in vivo* approaches were both applied to reveal a novel function of Foxc1 on microglia-mediated inflammatory response, migration and neuronal apoptosis during sepsis-induced cognitive dysfunction. The present study also provided evidence that Foxc1 can negatively

regulate the microglia-mediated inflammatory response, microglial migration and neuronal apoptosis through the NF-κB pathway. The adds support for the future therapeutic targeting of Foxc1 for the treatment of sepsis-related cognitive dysfunction in SAE.

In summary, CLP surgery induced-sepsis caused inflammatory responses in the hippocampus mediated by microglia, resulting in deficits of cognitive function. Foxc1 overexpression prevented sepsis-induced neuroinflammation, microglial migration, neuronal apoptosis and cognitive dysfunction, which was likely mediated through its effects on IκBα and NF-κB signaling. Therefore, targeting Foxc1/IκBα signaling may serve as a viable therapeutic strategy for treating or preventing cognitive dysfunction in SAE.

Acknowledgements

Not applicable.

Funding

The present study was supported by Chinese International Medical Exchange Foundation 2021 (grant no. Z-2016-23-2101-37), Cardiovascular Multidisciplinary Integrated Thinking Research Fund (grant no. z-2016-23-2101-37) and Key Scientific Research Project Plan of Henan University (grant no. 20A320007).

Availability of data and materials

The datasets used and/or analyzed during the current study are available from the corresponding author on reasonable request.

Authors' contributions

Hongyu W conducted most of the experiments and drafted the manuscript. YS, CL and XQ made substantial contributions to data analysis and data interpretation. DZ and XJ were involved in performing some of the experiments and data analysis. Hongwei W and SZ made substantial contributions to conception and design, were involved in revising the manuscript critically for important intellectual content, and gave their final approval of the published version. All authors read and approved the final version of the manuscript. Hongyu W and Hongwei W confirmed the authenticity of all the raw data.

Ethics approval and consent to participate

All study procedures were approved by the Institutional Animal Care and Use Committee of Shanghai Jiao Tong University School of Medicine (approval no. XHEC-F-2019-030; Shanghai, China).

Patient consent for publication

Not applicable.

Competing interests

The authors declare that they have no conflict of interests.

References

1. Gofton TE and Young GB: Sepsis-associated encephalopathy. Nat Rev Neurol 8: 557-566, 2012.
2. Czempik PF, Pluta MP and Krzych ŁJ: Sepsis-associated brain dysfunction: A review of current literature. Int J Environ Res Public Health 17: 5852, 2020.
3. Sonneville R, de Montmollin E, Poujade J, Garrouste-Orgeas M, Souweine B, Darmon M, Mariotte E, Argaud L, Barbier F, Goldgran-Toledano D, *et al*: Potentially modifiable factors contributing to sepsis-associated encephalopathy. Intensive Care Med 43: 1075-1084, 2017.
4. Abe N, Nishihara T, Yorozuya T and Tanaka J: Microglia and macrophages in the pathological central and peripheral nervous systems. Cells 9: 2132, 2020.
5. Michels M, Abatti M, Vieira A, Ávila P, Goulart AI, Borges H, Córneo E, Dominguini D, Barichello T and Dal-Pizzol F: Modulation of microglial phenotypes improves sepsis-induced hippocampus-dependent cognitive impairments and decreases brain inflammation in an animal model of sepsis. Clin Sci (Lond) 134: 765-776, 2020.
6. Wang LM, Wu Q, Kirk RA, Horn KP, Ebada Salem AH, Hoffman JM, Yap JT, Sonnen JA, Towner RA, Bozza FA, *et al*: Lipopolysaccharide endotoxemia induces amyloid-β and p-tau formation in the rat brain. Am J Nucl Med Mol Imaging 8: 86-99, 2018.
7. Gunther ML, Morandi A, Krauskopf E, Pandharipande P, Girard TD, Jackson JC, Thompson J, Shintani AK, Geevarghese S, Miller RR III, *et al*: The association between brain volumes, delirium duration, and cognitive outcomes in intensive care unit survivors: The VISIONS cohort magnetic resonance imaging study*. Crit Care Med 40: 2022-2032, 2012.
8. Adam N, Kandelman S, Mantz J, Chrétien F and Sharshar T: Sepsis-induced brain dysfunction. Expert Rev Anti Infect Ther 11: 211-221, 2013.
9. Maddux AB, Hiller TD, Overdier KH, Pyle LL and Douglas IS: Innate immune function and organ failure recovery in adults with sepsis. J Intensive Care Med 34: 486-494, 2019.
10. Dal-Pizzol F, Tomasi CD and Ritter C: Septic encephalopathy: Does inflammation drive the brain crazy? Braz J Psychiatry 36: 251-258, 2014.
11. Michels M, Vieira AS, Vuolo F, Zapelini HG, Mendonça B, Mina F, Dominguini D, Steckert A, Schuck PF, Quevedo J, *et al*: The role of microglia activation in the development of sepsis-induced long-term cognitive impairment. Brain Behav Immun 43: 54-59, 2015.
12. Margotti W, Giustina AD, de Souza Goldim MP, Hubner M, Cidreira T, Denicol TL, Joaquim L, De Carli RJ, Danielski LG, Metzker KL, *et al*: Aging influences in the blood-brain barrier permeability and cerebral oxidative stress in sepsis. Exp Gerontol 140: 111063, 2020.
13. Shulyatnikova T and Verkhratsky A: Astroglia in sepsis associated encephalopathy. Neurochem Res 45: 83-99, 2020.
14. Zhang SP, Yang RH, Shang J, Gao T, Wang R, Peng XD, Miao X, Pan L, Yuan WJ, Lin L and Hu QK: FOXC1 up-regulates the expression of toll-like receptors in myocardial ischaemia. J Cell Mol Med 23: 7566-7580, 2019.
15. Xia W, Zhu J, Wang X, Tang Y, Zhou P, Wei X, Chang B, Zheng X, Zhu W, Hou M and Li S: Overexpression of Foxc1 regenerates crushed rat facial nerves by promoting Schwann cells migration via the Wnt/β-catenin signaling pathway. J Cell Physiol 235: 9609-9622, 2020.
16. Liu J, Zhang Z, Li X, Chen J, Wang G, Tian Z, Qian M, Chen Z, Guo H, Tang G, *et al*: Forkhead box C1 promotes colorectal cancer metastasis through transactivating ITGA7 and FGFR4 expression. Oncogene 37:5477-5491, 2018.
17. Xia S, Qu J, Jia H, He W, Li J, Zhao L, Mao M and Zhao Y: Overexpression of Forkhead box C1 attenuates oxidative stress, inflammation and apoptosis in chronic obstructive pulmonary disease. Life Sci 216: 75-84, 2019.
18. Zhao L, Zhang R, Su F, Dai L, Wang J, Cui J, Huang W and Zhang S: FoxC1-induced vascular niche improves survival and myocardial repair of mesenchymal stem cells in infarcted hearts. Oxid Med Cell Longev 2020: 7865395, 2020.
19. Cao Q, Wang X, Shi Y, Zhang M, Yang J, Dong M, Mi Y, Zhang Z, Liu K, Jiang L, *et al*: FOXC1 silencing inhibits the epithelial-to-mesenchymal transition of glioma cells: Involvement of β-catenin signaling. Mol Med Rep 19: 251-261, 2019.

20. Nishimura DY, Swiderski RE, Alward WL, Searby CC, Patil SR, Bennet SR, Kanis AB, Gastier JM, Stone EM and Sheffield VC: The forkhead transcription factor gene FKHL7 is responsible for glaucoma phenotypes which map to 6p25. Nat Genet 19: 140-147, 1998.
21. Huang L, Huang Z, Fan Y, He L, Ye M, Shi K, Ji B, Huang J, Wang Y and Li Q: FOXC1 promotes proliferation and epithelial-mesenchymal transition in cervical carcinoma through the PI3K-AKT signal pathway. Am J Transl Res 9: 1297-1306, 2017.
22. Ray PS, Wang J, Qu Y, Sim MS, Shamonki J, Bagaria SP, Ye X, Liu B, Elashoff D, Hoon DS, *et al*: FOXC1 is a potential prognostic biomarker with functional significance in basal-like breast cancer. Cancer Res 70: 3870-3876, 2010.
23. Omatsu Y, Seike M, Sugiyama T, Kume T and Nagasawa T: Foxc1 is a critical regulator of haematopoietic stem/progenitor cell niche formation. Nature 508: 536-540, 2014.
24. Hayden MS and Ghosh S: Shared principles in NF-kappaB signaling. Cell 132: 344-362, 2008.
25. Dolcet X, Llobet D, Pallares J and Matias-Guiu X: NF-kB in development and progression of human cancer. Virchows Arch 446: 475-482, 2005.
26. Nguyen PL, Bui BP, Lee H and Cho J: A Novel 1,8-Naphthyridine-2-carboxamide derivative attenuates inflammatory responses and cell migration in LPS-Treated BV2 Cells via the suppression of ROS generation and TLR4/Myd88/NF-κB signaling pathway. Int J Mol Sci 22: 2527, 2021.
27. Campesi I, Montella A and Franconi F: Human monocytes respond to lipopolysaccharide (LPS) stimulation in a sex-dependent manner. J Cell Physiol: Jul 12, 2021 (Epub ahead of print). doi: 10.1002/jcp.30503.
28. National Research Council Institute for Laboratory Animal R: In: Guide for the Care and Use of Laboratory Animals National Academies Press (US) Copyright 1996 by the National Academy of Sciences. Washington, DC, 1996.
29. Yin J, Shen Y, Si Y, Zhang Y, Du J, Hu X, Cai M, Bao H and Xing Y: Knockdown of long non-coding RNA SOX2OT downregulates SOX2 to improve hippocampal neurogenesis and cognitive function in a mouse model of sepsis-associated encephalopathy. J Neuroinflammation 17: 320, 2020.
30. Gao H, Han Z, Huang S, Bai R, Ge X, Chen F and Lei P: Intermittent hypoxia caused cognitive dysfunction relate to miRNAs dysregulation in hippocampus. Behav Brain Res 335: 80-87, 2017.
31. Shan G, Tang T, Xia Y and Qian HJ: Long non-coding RNA NEAT1 promotes bladder progression through regulating miR-410 mediated HMGB1. Biomed Pharmacother 121: 109248, 2020.
32. Livak KJ and Schmittgen TD: Analysis of relative gene expression data using real-time quantitative PCR and the 2(-Delta Delta C(T)) Method. Methods 25: 402-408, 2001.
33. Wang H, Yang T, Sun J, Zhang S and Liu S: SENP1 modulates microglia-mediated neuroinflammation toward intermittent hypoxia-induced cognitive decline through the de-SUMOylation of NEMO. J Cell Mol Med 25: 6841-6854, 2021.
34. Wang J, Ray PS, Sim MS, Zhou XZ, Lu KP, Lee AV, Lin X, Bagaria SP, Giuliano AE and Cui X: FOXC1 regulates the functions of human basal-like breast cancer cells by activating NF-κB signaling. Oncogene 31: 4798-4802, 2012.
35. Huang W, Chen Z, Zhang L, Tian D, Wang D, Fan D, Wu K and Xia L: Interleukin-8 induces expression of FOXC1 to promote transactivation of CXCR1 and CCL2 in hepatocellular carcinoma cell lines and formation of metastases in mice. Gastroenterology 149: 1053-1067.e14, 2015.
36. Chen Z and Trapp BD: Microglia and neuroprotection. J Neurochem 136 (Suppl 1): S10-S17, 2016.
37. Kettenmann H, Hanisch UK, Noda M and Verkhratsky A: Physiology of microglia. Physiol Rev 91: 461-553, 2011.
38. Colonna M and Butovsky O: Microglia function in the central nervous system during health and neurodegeneration. Annu Rev Immunol 35: 441-468, 2017.
39. Vaessen TJ, Overeem S and Sitskoorn MM: Cognitive complaints in obstructive sleep apnea. Sleep Med Rev 19: 51-58, 2015.
40. Kiernan EA, Smith SMC, Mitchell GS and Watters JJ: Mechanisms of microglial activation in models of inflammation and hypoxia: Implications for chronic intermittent hypoxia. J Physiol 594: 1563-1577, 2016.
41. de Lima FFF, Mazzotti DR, Tufik S and Bittencourt L: The role inflammatory response genes in obstructive sleep apnea syndrome: A review. Sleep Breath 20: 331-338, 2016.
42. Calsolaro V and Edison P: Neuroinflammation in Alzheimer's disease: Current evidence and future directions. Alzheimers Dement 12: 719-732, 2016.
43. Yang Q, Wang Y, Feng J, Cao J and Chen B: Intermittent hypoxia from obstructive sleep apnea may cause neuronal impairment and dysfunction in central nervous system: The potential roles played by microglia. Neuropsychiatr Dis Treat 9: 1077-1086, 2013.
44. Zhai Q, Li F, Chen X, Jia J, Sun S, Zhou D, Ma L, Jiang T, Bai F, Xiong L and Wang Q: Triggering receptor expressed on myeloid cells 2, a novel regulator of immunocyte phenotypes, confers neuroprotection by relieving neuroinflammation. Anesthesiology 127: 98-110, 2017.
45. Xia CY, Zhang S, Gao Y, Wang ZZ and Chen NH: Selective modulation of microglia polarization to M2 phenotype for stroke treatment. Int Immunopharmacol 25: 377-382, 2015.
46. Hellström Erkenstam N, Smith PL, Fleiss B, Nair S, Svedin P, Wang W, Boström M, Gressens P, Hagberg H, Brown KL, *et al*: Temporal characterization of microglia/macrophage phenotypes in a mouse model of neonatal hypoxic-ischemic brain injury. Front Cell Neurosci 10: 286, 2016.
47. Dou Y, Wu HJ, Li HQ, Qin S, Wang YE, Li J, Lou HF, Chen Z, Li XM, Luo QM and Duan S: Microglial migration mediated by ATP-induced ATP release from lysosomes. Cell Res 22: 1022-1033, 2012.
48. Mitchell S, Vargas J and Hoffmann A: Signaling via the NF-κB system. Wiley Interdiscip Rev Syst Biol Med 8: 227-241, 2016.
49. Viatour P, Merville MP, Bours V and Chariot A: Phosphorylation of NF-kappaB and IkappaB proteins: Implications in cancer and inflammation. Trends Biochem Sci 30: 43-52, 2005.
50. Chen S, Tang C, Ding H, Wang Z, Liu X, Chai Y, Jiang W, Han Y and Zeng H: Maf1 ameliorates sepsis-associated encephalopathy by suppressing the NF-κB/NLRP3 inflammasome signaling pathway. Front Immunol 11: 594071, 2020.
51. Matthew SH and Sankar G: Shared principles in NF-kappaB signaling. Cell 132: 344-362, 2008.
52. Oliver KM, Garvey JF, Ng CT, Veale DJ, Fearon U, Cummins EP and Taylor CT: Hypoxia activates NF-kappaB-dependent gene expression through the canonical signaling pathway. Antioxid Redox Signal 11: 2057-2064, 2009.
53. Regen F, Hellmann-Regen J, Costantini E and Reale M: Neuroinflammation and Alzheimer's Disease: Implications for microglial activation. Curr Alzheimer Res 14: 1140-1148, 2017.
54. Ho MS: Microglia in Parkinson's Disease. Adv Exp Med Biol 1175: 335-353, 2019.
55. Bjelobaba I, Savic D and Lavrnja I: Multiple sclerosis and neuroinflammation: The overview of current and prospective therapies. Curr Pharm Des 23: 693-730, 2017.
56. Hong S, Beja-Glasser VF, Nfonoyim BM, Frouin A, Li S, Ramakrishnan S, Merry KM, Shi Q, Rosenthal A, Barres BA, *et al*: Complement and microglia mediate early synapse loss in Alzheimer mouse models. Science 352: 712-716, 2016.
57. Wang H, Xiong W, Hang S, Wang Y, Zhang S and Liu S: Depletion of SENP1-mediated PPARγ SUMOylation exaggerates intermittent hypoxia-induced cognitive decline by aggravating microglia-mediated neuroinflammation. Aging (Albany NY) 13: 15240-15254, 2021.